Available online at www.sciencedirect.com
SCIENCE DIRECT
Spectrochimica Acta Part A 63 (2006) 518–523
SPECTROCHIMICA ACTA PART A
www.elsevier.com/locate/saa

Synthesis and spectroscopic study of copper(II) and manganese(II) complexes with pipemidic acid

Beata Szymańska [a], Danuta Skrzypek [a,*], Dimitra Kovala-Demertzi [b,*], Malgorzata Staninska [b], Mavroudis A. Demertzis [b]

[a] *A. Chełkowski Institute of Physics, University of Silesia, Uniwersytecka 4, 40-007 Katowice, Poland*
[b] *Section of Inorganic and Analytical Chemistry, Department of Chemistry, University of Ioannina, Ioannina 45110, Greece*

Received 8 March 2005; received in revised form 23 May 2005; accepted 24 May 2005

Abstract

The interaction of copper(II) and manganese(II) with pipemidic acid, Hpipem, afforded the complexes $[Cu(pipem)_2(H_2O)]\cdot 2H_2O$, **1** and $[Mn(pipem)_2(H_2O)]$, **2**. The new complexes have been characterised by elemental analyses, infrared, UV–vis and X-band EPR spectroscopy in the temperature range from 4 to 300 K. The monoanion, pipem, exhibits *O,O* ligation through the carbonyl and carboxylato oxygen atoms. Five coordinate square-pyramid configuration has been proposed for **1** and **2**, and the fifth apical position is occupied by a coordinated water molecule.

Keywords: Pipemidic acid (HPipem); Cu(II) and Mn(II) complexes; EPR

1. Introduction

Pipemidic acid [8-Ethyl-5,8-dihydro-5-oxo-2-(1-piperazinyl)-pyrido(2,3-d)pyrimidine-6-carboxylic acid trihydrate], $Hpipem\cdot 3H_2O$, belongs to the group of compounds known as quinolones, which is one of most important group of synthetic, antibacterial agents structurally related to nalidixic acid. Quinolones, represented by nalidixic, oxolinic and pipemidic acids, are employed as specific inhibitors of the bacterial DNA-gyrase, the enzyme responsible for converting double-stranded DNA into a negative superhelical form. The introduction of a piperazinyl side chain at position 7 (to provide pipemidic acid) has been shown to increase the ability of the quinolones to penetrate the bacterial cell wall, thus enhancing activity. Hpipem was found effective against some organisms resistant to piromidic or nalidixic acids [1–3].

X-ray crystal structure of $Hpipem\cdot 3H_2O$ revealed that the carboxylic group is ionized and the molecule exists in a zwitterionic form with protonated terminal nitrogen of the piperazine ring, Fig. 1 [4]. It was suggested that the ability of the drug to penetrate into cells is a function of its net charge and in zwitterionic form exhibits maximum permeation properties [5]. The interaction of metal ions with drugs administered for therapeutic purposes is a subject of considerable interest [7]. The interactions of metal ions with quinolone antibacterial agents have been reviewed [5] and the crystal structure of cinoxacin has been found [6]. Synthesis, characterization, and antibacterial activities of some rare earth metal complexes of pipemidic acid have been referred [8]

In this paper, we report the syntheses and spectral characterization of the novel complexes $[Cu(pipem)_2(H_2O)]\cdot 2H_2O$, **1** and $[Mn(pipem)_2(H_2O)]$, **2**.

2. Experimental

2.1. General considerations

The reagents (Aldrich, Merck) were used as supplied, while the solvents were purified according to standard pro-

* Corresponding authors. Tel.: +30 2651098425; fax: +30 2651098791.
E-mail addresses: dskrzyp@us.edu.pl (D. Skrzypek), dkovala@cc.uoi.gr (D. Kovala-Demertzi).

1386-1425/$ – see front matter © 2005 Elsevier B.V. All rights reserved.
doi:10.1016/j.saa.2005.05.038

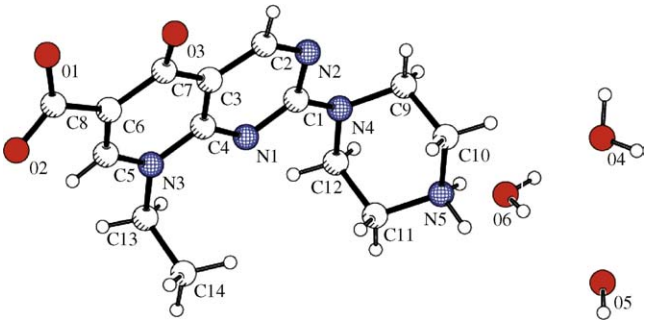

Fig. 1. The zwitterionic form of Hpipem·3H_2O [4].

cedures. Pipemidic acid was a gift from Farmaceutici Damor S.p.A. C, H and N analyses were carried out by the microanalytical service of the University of Ioannina. Melting points were determined in open capillaries and are uncorrected. Infrared and far-infrared spectra were recorded on a Nicolet 55XC Fourier transform spectrophotometer using KBr pellets (4000–400 cm^{-1}) and nujol mulls dispersed between polyethylene disks (400–40 cm^{-1}). Ligand-field spectra were obtained on a Perkin–Elmer Lambda 900 spectrophotometer using the diffuse reflectance technique, with MgO as a reference. The X-ray powder diffraction (XRD) analysis was carried out with the use of Siemens D5000 diffraction equipment. The filtered Cu K_α radiation was selected and the scans were recorded in a (5°–100°), 2θ range.

2.2. Synthesis of the complexes

2.2.1. Synthesis of [Cu(pipem)$_2$(H_2O)]·2H_2O (**1**)

A solution of [$Cu(CH_3COO)_2$]H_2O (0.0998 g, 0.5 mmol) in methanol (5 ml) was added to a solution of pipemidic acid (0.303 g, 1 mmol) in methanol (25 ml). Drops of triethylamine ($N(eth)_3$) were added till the apparent pH value was ∼7. The reaction mixture was stirred at room temperature for 2 h and cooled to 5 °C in a refrigerator for 4 h. The precipitate was collected by filtration, washed with cold methanol and diethyl ether and dried in vacuo to afford (**1**) (green powder 70% yield). Anal. Calc. for $C_{28}H_{38}CuN_{10}O_9$: C, 46.57; H, 5.30; N, 19.40; Found: C, 46.47; H, 5.40; N, 19.20%. IR (KBr, cm^{-1}): ν(OH), 3422 (br s), 3206 (ms); ν(NH), 2973 (m), 3045 (m); ν(CH), 2938 (m); ν(CH_2), 2742 (m); ν(C=O), 1626 (s); ν_{asym}(COO), 1604 (s); ν_{sym}(COO), 1361 (s); ν(C=N), 1570 (ms); ν(M–O_{H_2O}), 395 (sh); ν(M–$O_{c=o}$), 361 (ms); ν(M–O_{oco}), 300 (ms). UV–vis, reflectance spectrum, for **1**: 745 nm, 350 nm.

2.2.2. Synthesis of [Mn(pipem)$_2$(H_2O)] (**2**)

A solution of $MnCl_2$ (0.0315 g, 0.25 mM) in methanol (2.5 ml) was added to a solution of pipemidic acid (0.1515 g, 0.5 mM) in methanol (5 ml). Drops of triethylamine ($N(eth)_3$) were added till the apparent pH value was ∼7. The reaction mixture was stirred at room temperature for 2 h and cooled to 5 °C in a refrigerator for 4 h. The precipitate was collected by filtration, washed with cold methanol and dried in vacuo to afford (**2**) (yellow powder 80% yield). Anal. Calc. for $C_{28}H_{34}CuN_{10}O_7$: C, 49.64; H,5.05; N, 20.67; Found: C, 49.50; H, 5.20; N, 20.02%. IR (cm^{-1}): ν(OH), 3431 (br s); ν(NH), 3053 (m); ν(CH), 2936 (m); ν(CH2), 2791 (m); ν(C=O), 1629 (s); ν_{asym}(COO), 1614 (s); ν_{sym}(COO), 1362 (s); ν(C=N), 1572 (ms); ν(M–O_{H_2O}), 393 (ms); ν(M–$O_{c=o}$), 372 (ms); ν(M–O_{oco}), 301 (ms). UV–vis, reflectance spectrum, for **2**: 405sh nm, 340 nm.

2.3. EPR spectroscopy

Electron paramagnetic resonance spectra of Cu(II) and Mn(II) complexes of Hpipem were recorded on Radiopan SE/X spectrometer with TE_{102} rectangular cavity and 100 kHz field modulation, equipped with an Oxford Instruments ESR 910 helium flow cryostat. The microwave frequency was measured using Hewlett Packard 534 microwave frequency counter and the magnetic field strength was monitored by a NMR teslameter. The temperature dependence measurements were performed in the temperature range from 4 to 300 K for powder samples and from 100 to 263 K for frozen aqueous solution. The measurements were carried out on solutions degassed and sealed under vacuum to eliminate the line broadening from dissolved oxygen. All EPR parameters were confirmed by simulation using Bruker-Symphonia software package.

3. Results and discussion

3.1. IR and UV–vis spectra

The complexes **1** and **2** were prepared in methanol solutions in the molar ratio 1:2. The complexes of pipem **1** and **2** were synthesized in powder form. The X-ray diffraction data indicate that **1** and **2** are poorly crystallised, Fig. 1. The complexes are stable in atmospheric conditions, slight soluble (**1**) and soluble (**2**) in water and insoluble in polar and non-polar organic solvents, nitromethane, cyclohexane, Me_2CO, $CHCl_3$, CH_3CN, CH_2Cl_2, MeOH, EtOH, DMSO and DMF. The elemental analyses confirm their stoichiometry. IR and UV–Vis spectroscopic studies were used to probe the metal–ligand environment for the two complexes.

The IR spectra of Hpipem·3H_2O do not have a ν(C=O) absorption [5], according to the crystal structure of Hpipem, where the carboxylic group is deprotonated and the molecule exists in zwitterionic form [4]. It is known that ionic carboxylates [5] show no carbonyl stretching at about 1700 cm^{-1}, but have two characteristic bands in the range of 1650–1510 cm^{-1} and 1400–1280 cm^{-1} that could be assigned as ν_{asym} and ν_{sym} (COO) stretching vibrations. As the carboxyl hydrogen is more acidic than the amino hydrogen the deprotonation occurs in the carboxylic group. This is confirmed by the IR spectra of the complexes, showing the characteristic bands for the secondary amino groups and for the coordinated carboxylato group. The IR of

Hpipem·3H_2O, **1** and **2** gave band at 3021, 2973, 3045 and 3053 cm^{-1} attributable to intra- or inter-molecular NH···O hydrogen bonds. A broad absorption at ∼3400 cm^{-1} in the spectra of the complexes was attributed to the presence of coordinated water. In the solid state, the infrared spectrum of **1** exhibits bands at 3422 and 3206 cm^{-1}, attributed to the presence of coordinated and lattice water, respectively [9]. The ν_{asym}(COO) and ν_{sym}(COO) bands appear at 1614–1604 and at 1360–1362 cm^{-1}, respectively. The difference, $\Delta[\nu_{asym}(COO) - \nu_{sym}(COO)]$ between these frequencies is 243 and 252 for **1** and **2** respectively. These values are consistent with monodentate coordination of the carboxylato group [10]. The band at ∼1570 cm^{-1}, 1574 for Hpipem·3H_2O, 1570 for **1** and 1572 cm^{-1} for **2**, is assigned to ν(C=N) mode. The non-ligand bands in the regions 390–395, 361–375 and 300–301 cm^{-1} are tentatively assigned to ν(M–O_{H2O}), ν(M–$O_{c=o}$) and ν(M–O_{oco}) modes, respectively [11]. These data indicate coordination through the oxygen atoms of the carboxylato group, carbonyl group and water molecule and no interaction between the endocyclic nitrogens (C=N) and metal ions.

3.2. EPR spectra of Cu(II)–pipemidic acid complex

EPR spectra of **1** in solid state at selected temperatures are shown in Fig. 2. The spectra exhibit anisotropic signal with a poorly resolved hyperfine structure in a wide temperature range.

The result of our experiment can be explained using the model of EPR spectra in a Jahn–Teller disorder system described by Cantin et al. [12]. This model is based on a statistical distribution of the energy difference between the lowest and the two higher potential energy minima of the Jahn–Teller centre in a low-symmetry host site. The disorder of **1** is related to a poor crystallisation of sample (Fig. 3). The presence of copper(II) ions in the disordered materials resulted in an EPR spectrum. They showed a significant g and A strain, consisting of a progressive broadening and decrease in the intensity of the hyperfine lines as the order of m_I increases in the low field part of the spectrum ($I = 3/2$ is the Cu nuclear spin). Simultaneously, a common feature for glassy and disordered systems is the broadness of their absorption lines. This is usually associated with the randomness of these structures and a distribution of the EPR parameters around some average values due to small variations in the local geometry of the site [13]. The EPR spectra of the complex **1** were interpreted in terms of the following spin-Hamiltonian [14]:

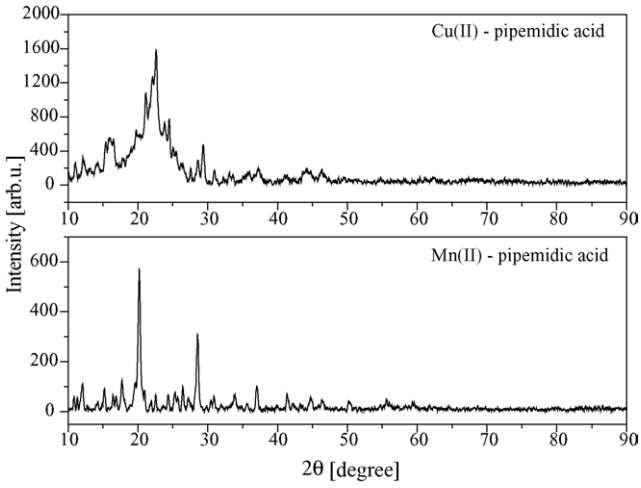

Fig. 2. X-ray diffraction pattern of the Cu(II)– and Mn(II)– pipemidic acid complexes.

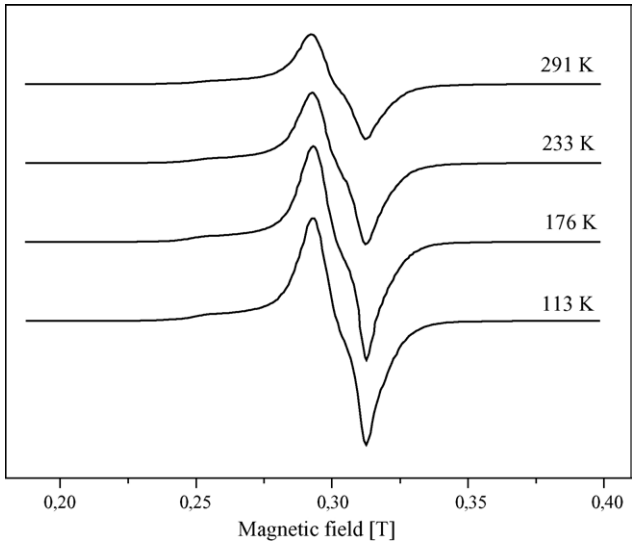

Fig. 3. The EPR spectra of solid copepr(II)–pipemidic acid complex at selected temperatures.

$$H = \mu_B(g_z B_z S_z + g_x B_x S_x + g_y B_y S_y) + A_z I_z S_z \quad (1)$$

The values for the spin-Hamiltonian parameters were determined on the basis of the best fit for the simulated spectra as compared with the experimentally observed spectra (see Fig. 4). These EPR parameters are listed in Table 1 Copper(II) centres exhibit a distorted square pyramid structure, Table 1, with ground state [15]:

$$a|x^2 - y^2\rangle + b|z^2\rangle \quad a^2 + b^2 = 1 \quad (2)$$

The g-factors of copper(II) complexes for rhombic symmetry may be expressed by [15]:

$$g_z = 2\left\{1 - 4\left(\frac{\lambda}{E_{xy}}\right)a^2\right\};$$

$$g_y = 2\left\{1 - \left(\frac{\lambda}{E_{yz}}\right)(a + 1.7b)^2\right\};$$

$$g_x = 2\left\{1 - \left(\frac{\lambda}{E_{xz}}\right)(a - 1.7b)^2\right\} \quad (3)$$

where E_{xy} and E_{xz}, E_{yz} are the electron transition energies of $^2B_{1g} \rightarrow {}^2B_{2g}$ and $^2B_{1g} \rightarrow {}^2E_g$, respectively. The energy level sequence will depend on the amount of distortion due to the ligand field and the Jahn–Teller effect. The values of a and b factors, Table 1, which are a measure of covalency were

Table 1
EPR and bonding parameters of copper(II)–pipemidic acid complex

Complex: $[Cu(pipem)_2(H_2O)]\cdot 2H_2O$ $T = 113$ K											
g_x	g_y	g_z	$A_z \times 10^{-4}$ (cm^{-1})	ΔB_x (mT)	ΔB_y (Mt)	ΔB_z (mT)	f (cm)	a	b	α^2	β_1^2
2.062	2.174	2.320	165	3	4.5	15	140	0.81	0.59	0.86	0.76

calculated from relations (3) with the help of the optical data. Approximate metal–ligand σ-bond coefficient (α^2) which is defined as the fraction of unpaired electron density located on the copper ion was calculated from Kivelson and Neiman form [16]:

$$\alpha^2 = -\left(\frac{A_\parallel}{P}\right) + (g_\parallel - 2) + \frac{3}{7}(g_\perp - 2) + 0.04 \qquad (4)$$

The obtained α^2 value (see Table 1) confirmed considerable covalency in the bonding between the Cu(II) ion and the ligand. From the a-value we calculated β_1^2, which is a direct measure of the covalency of the in-plane π bonding.

The f value of **1** is 140 cm and implies the presence of distorted structure. The characteristic linear dependence of $A_\parallel$ on $g_\parallel$ for the complexes formed between Cu(II) and similar donor atoms provides an important possibility for discrimination between N_4, O_3N_1, O_2N_2, O_1N_3 and N_4 donor sets in xy plane. The variation in $g_\parallel$ and $A_\parallel$ of the copper(II) complexes with the similar donor atoms is caused by the change in overall charge of the complex [17]. The values of these parameters summarised in Table 1 mean the coordination of four oxygen atoms around Cu(II) in the plane xy.

The magnetic properties of investigated copper (II) complex were checked by EPR measurements in temperature range from 4 to 300 K. In Fig. 5 temperature evolution of EPR intensity (calculated as double integration of the spectrum—DI) of complex **1** is shown. Thus defined intensity is proportional to the spin susceptibility of the sample. It

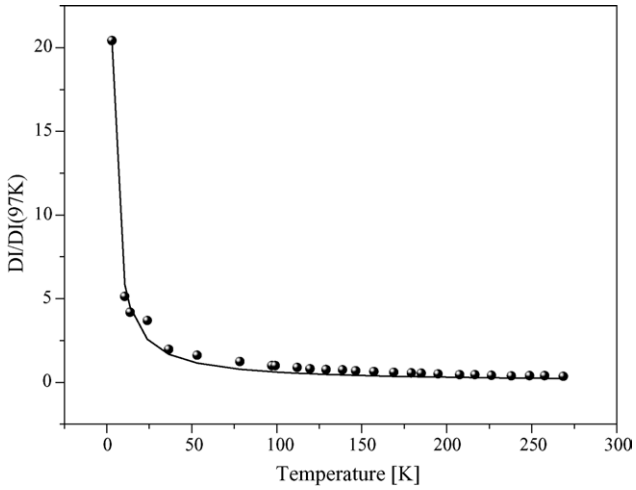

Fig. 5. The temperature dependence of spin susceptibility for **1** (the solid line is calculated using Curie law).

was established that the spin susceptibility of **1** follows the Curie law (the solid line in Fig. 5).

3.3. EPR spectra of Mn(II)–pipemidic acid complex

The EPR spectrum of powder Mn(II)–pipemidic acid complex consists of the strong signal with the Lorentzian shape with linewidth $\Delta B = 17$ mT, centred around $g = 2$ without any changes in whole temperature range, Fig. 6 It is known,

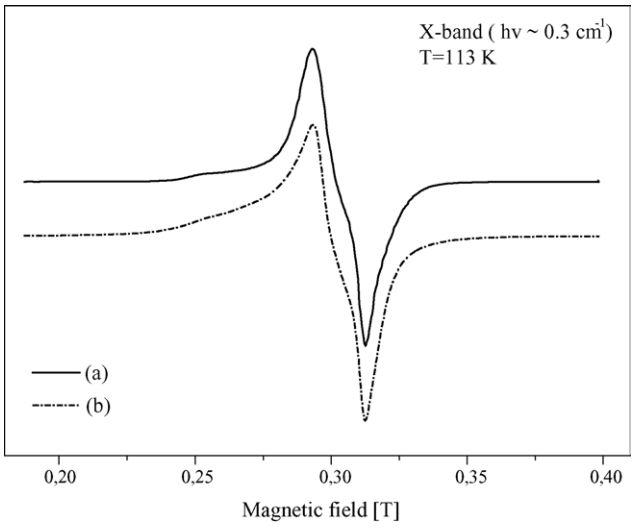

Fig. 4. X-band EPR spectrum of complex **1** at $T = 113$ K; (a) experimental spectrum; (b) simulated spectrum (the simulation was obtained using the parameters in Table 1).

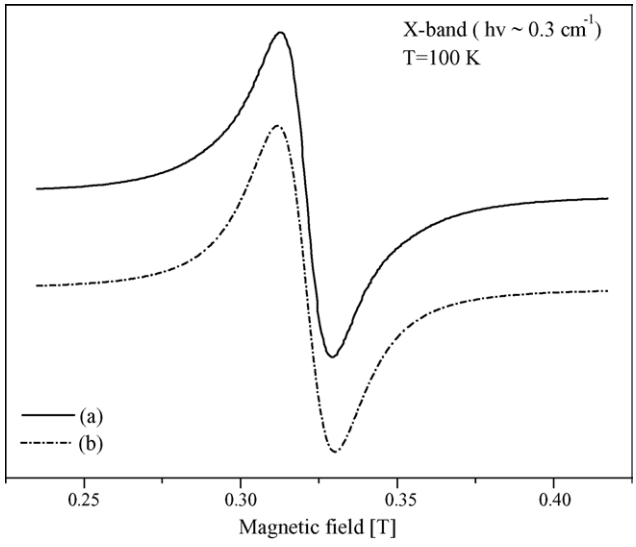

Fig. 6. X-band EPR spectrum of **2** at $T = 100$ K; (a) experimental spectrum; (b) simulated spectrum (the simulation was obtained using the parameters in Table 2).

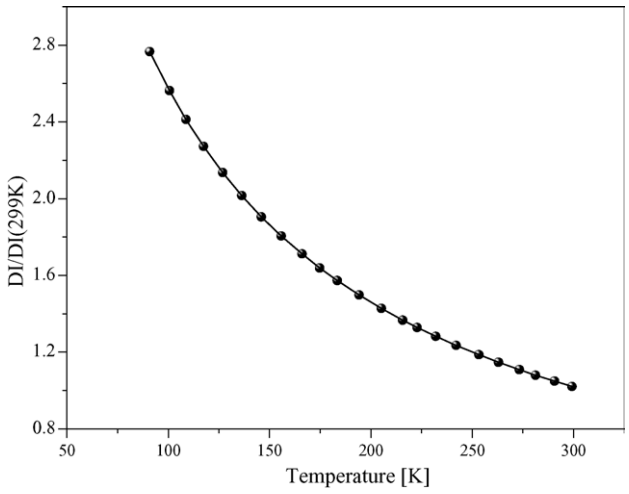

Fig. 7. The temperature dependence of spin susceptibility for **2** complex; the solid line iscalculated using Curie–Weiss law.

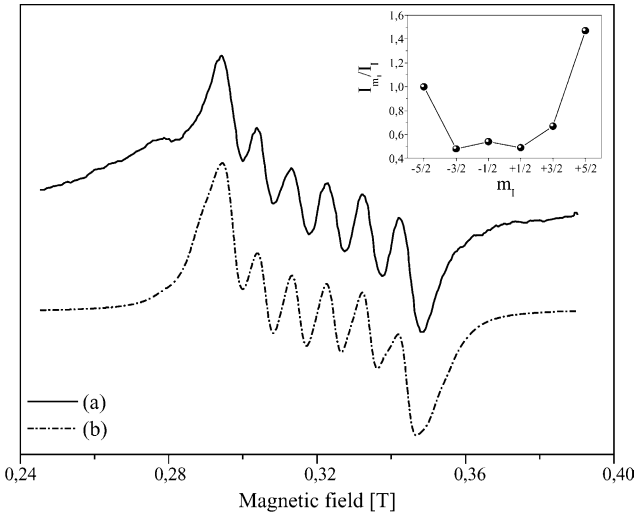

Fig. 8. The EPR spectrum of frozen solution of complex **2**; (a) experimental spectrum; (b) simulated spectrum (the simulation was obtained using the parameters in Table 2).

that a system consisting of many identical ions coupled by exchange interactions gives an isotropic Lorentzian spectrum centred near the *g*-value of the isolated ion without fine and hyperfine structures [14]. Dowsing et al [18] observed this spectrum for different manganese complexes.

The features of spectra presented in Fig. 6 mean that dipole–dipole and exchange interactions are present in the complex **2**. These spectra can be interpreted using theory of narrowing exchange which assumes that the exchange-induced fluctuations are sufficiently rapid to average the dipolar field and describes a linewidth according to the following equation [14]:

$$\Delta\omega \approx \frac{\omega_{\mathrm{P}}^2}{\omega_{\mathrm{ex}}} \tag{5}$$

where: $\Delta\omega$ is the linewidth in frequency units; ω_{ex} is the frequency associated with isotropic exchange; ω_{p} includes the contributions due to anisotropic interactions: dipolar, crystal-field, antisymmetric exchange, etc.

The changes of spin susceptibility measured as temperature dependence of DI (DI is the intensity calculated as double integration of spectrum) is a confirmation of the presence of magnetic interactions in powder complex **2**. It was established that the spin susceptibility of complex **2** follows the Curie–Weiss law, Fig. 7 The antiferromagnetic character of interactions between manganese ions is revealed by negative Curie–Weiss temperature $\theta = -30$ K.

The EPR measurements of complex **2** in solution brought more detailed information about the coordination sphere of Mn(II) centre. The lines belonging to the central hyperfine sextet with a broad background signal underneath the sextet are observed to the frozen aqueous solution of **2**, Fig. 8(a). Simultaneously, a complete smearing of the hyperfine forbidden lines and a significant broadening of hyperfine allowed lines become visible. These are the characteristic features of Mn(II) EPR spectra in disordered systems [19]. They are due to the effects of distribution of D and E (ZFS) parameters around their average values. The spin Hamiltonian for Mn^{2+} ($S = 5/2$, $I = 5/2$) in low symmetric crystal field is given by [14]:

$$H = g\mu_{\mathrm{B}}\mathrm{BS}{+}\mathrm{AIS} + H_{\mathrm{ZFS}} \tag{6}$$

where all symbols have their usual meaning and H_{ZFS} is the zero-field splitting (ZFS) term. As Mn^{2+} is an S-state ion, the *g*- and *A*-tensors are isotropic.

The spectrum calculated with the best-fit EPR parameters, which are listed in Table 2 is shown in Fig. 8(b). The value of hyperfine coupling constant A may be analysed according to Jain and Lehmann review [20]. Parameter A of Mn(II) ions is decreased with increasing covalency of the magnetic complex. This relation was defined by plotting *A* versus the Pauling covalency parameter. The Pauling covalency parameter c/n is derived from the electronegativities of Mn^{2+} and the ligands, and n is the number of ligands at the nearest distance from the paramagnetic ion. From this dependence and from *A*-value obtained experimentally for complex **2** (see Table 2),

Table 2
EPR parameters of manganese(II)–pipemidic acid complex

Complex: $[Mn(pipem)_2(H_2O)]$					
	T (K)	g	ΔB (mT)	$A \times 10^{-4}(\mathrm{cm}^{-1})$	$D\ (\times 10^{-4}(\mathrm{cm}^{-1})$
Powder	112	2.000	17	–	–
Frozen solution	263	2.000	5	88	40

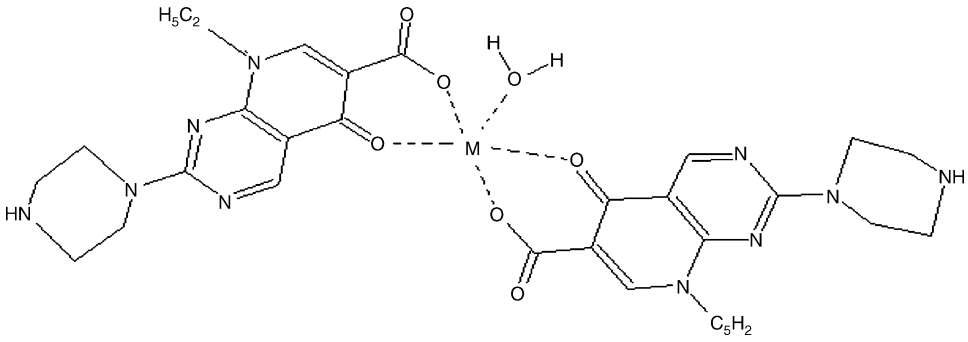

Fig. 9. The proposed structure of the mononuclear copper(II) and manganese(II) complexes of pipemidic acid.

we have concluded that Mn(II) in complex **2** is surrounded by oxygen ligands and the bond Mn(II)—O has slightly covalent character (about 10%).

At the same time, the information about the symmetry of the coordination sphere of Mn(II) in complex **2** may be extract from comparison of intensity of the components of the central hyperfine sextet. The inset in Fig. 8 shows the relative intensities of six lines as a function of m_I and exhibits a characteristic dip in the middle. This behaviour was explained by Eidels-Dubovoi et al. [21] where was used the perturbation theory method for obtaining the axial crystal-field parameter D in a disorder sample. The depth of dip is relative to the distortion of crystal field from octahedral symmetry. The calculations were made up to value about $D/B_0 = 0.044$, i.e. $D = 140 \times 10^{-4}\,cm^{-1}$ at X-band frequencies. The D-value was estimated from comparison of these results with calculations of relative intensities of EPR lines (see the inset in Fig. 8). The simulated spectrum obtained with the values $D = 40 \times 10^{-4}\,cm^{-1}$ and $A = 88 \times 10^{-4}\,cm^{-1}$ is shown in the Fig. 8(b). This result means axially symmetric local crystal-field around manganese(II) centre in the case of **2**.

4. Conclusions

From the overall study presented above it is concluded that the complexes **1** and **2** exhibit a five-coordinated configuration in a distorted square pyramid around the metal centre. The Cu(II) or Mn(II) ions are coordinated to four oxygen atoms (two oxygen atoms from two carboxylato groups and two oxygen atoms from two carbonyl groups) of the two pipem ligands and an oxygen atom of one water molecule occupying the apical position, resulting in a CuO_5 chromophore, Fig. 9 The values of EPR parameters obtained for **1** and **2** indicate that the local symmetry around paramagnetic centre is distorted and that only oxygen atoms are involved in the bonding between the metal ion and the ligands and confirm the optical spectroscopic studies.

References

[1] M. Shimizu, S. Nakamura, Y. Takase, N. Kurobe, Antimicrob. Agents Chemother. 7 (1975) 441.
[2] I.L.L. Shen, A.G. Pernet, Proc. Natl. Acad. Sci. USA 82 (1985) 307.
[3] P.C. Appelbaum, P.A. Hunter, Int. J. Antimicrob. Agents 16 (2000) 5–15.
[4] I. Fonseca, S. Martinej-Carrera, S. Garcia-Blanco, Acta Crystallogr. Sect. C (Cr. Str. Comm.) 42 (1986) 1618.
[5] I. Turel, Coord. Chem. Rev. 232 (2002) 27, and references therein.
[6] M. Ruiz, R. Ortzi, L. Perello, J. Latorre, J. Server-Carrio, J Inorg. Biochem. 65 (1997) 87, and references therein.
[7] D. Kovala-Demertzi, J. Inorg. Biochem. 79 (2000) 153.
[8] L. Yang, D. Tao, X. Yang, Y. Li, Y. Guo, Chem. Pharm. Bull. 51 (5) (2003) 494.
[9] D. Kovala-Demertzi, A. Galani, M.A. Demertzis, S. Skoulika, C. Kotoglou, J. Inorg. Biochem. 98 (2004) 358.
[10] V. Dokorou, M.A. Demertzis, J.P. Jasinski, D. Kovala-Demertzi, J. Organomet. Chem. 689 (2004) 317.
[11] D. Kovala-Demertzi, S.K. Hadjikakou, M.A. Demertzis, Y. Deligiannakis, J. Inorg. Biochem. 69 (1998) 223.
[12] Ch. Cantin, H. Daubric, J. Kliava, O. Kahn, Solid State Commn. 108 (1998) 17.
[13] S. Cannistrano, G. Giugliarelli, P. Marzola, F. Sacchetti, Solid St. Commn. 68 (1988) 369.
[14] A. Abragam, B. Bleaney, Electron Paramagnetic Resonance of Transition Ions, Clarendon Press, Oxford, 1970.
[15] S.K. Hoffmann, Acta Phys. Pol. A 49 (1976) 253.
[16] D. Kivelson, R. Neiman, J. Chem. Phys. 35 (1961) 149.
[17] U. Sakaguchi, A.W. Addison, J. Chem. Soc. Dalton Trans. (1979) 600.
[18] R.D. Dowsing, J.F. Gibson, D.M.L. Goodgame, M. Goodgame, P.J. Hayward, Nature 219 (1968) 1037.
[19] S.K. Misra, Physica B 203 (1994) 193.
[20] V.K. Jain, G. Lehmann, Phys. Stat. Sol. (b) 159 (1990) 495, and references therein.
[21] S. Eidels-Dubovoi, V. Beltran-Lopez, J. Mag. Res. 32 (1978) 441.